VI International Conference on Computational Bioengineering
ICCB 2015
M. Cerrolaza and S.Oller (Eds)

BLOOD FLOW ANALYSIS OF STA-MCA ANASTOMOSIS USING CFD

SHO TAKAYAMA[*1], MITSUYOSHI WATANABE[†2], HIROYUKI TAKAO[†2], DAHMANI CHIHEBEDDINE[†2,3], HIROYA MAMORI[†4] YUICHI MURAYAMA[†2] AND MAKOTO YAMAMOTO[†4]

[*1]Graduate School of Mechanical Engineering
Tokyo University of Science
6-3-1 Niijyuku, Katsushika-ku, Tokyo, 125-8585, Japan
e-mail: 4515632@ed.tus.ac.jp, www.rs.kagu.tus.ac.jp/yamamoto

[†2] Department of Neurosurgery
Jikei University School of Medicine
3-25-8 Nishishimbashi, Minato-ku, Tokyo, 105-8461, Japan
e-mail: takao@jikei.ac.jp, www.endovascular.jp

[†3] Siemens Japan K.K.
1-11-1 Gate-city Osaki West Tower, Osaki, Shinagawa-ku, Tokyo, 141-8644, Japan

[†4] Department of Mechanical Engineering
Tokyo University of Science
6-3-1 Niijuku, Katsushika-ku, Tokyo, 125-8585, Japan
e-mail: yamamoto@rs.kagu.tus.ac.jp, www.rs.kagu.tus.ac.jp/yamamoto

Key words: Computational Fluid Dynamics (CFD), stroke, STA-MCA anastomosis

Summary. *STA-MCA anastomosis is one of the operation remedies, which is known as a surgical cure for the stroke prevention. In this operation, the STA (Superficial Temporal Artery) is anastomosed to the MCA (Middle Cerebral Artery), and intended to perfuse the cerebral artery. However, this surgical form has no general criterion. Therefore, the surgeons perform the operations based on their experiences. To assess the effect of this operation, Computational Fluid Dynamics (CFD) is performed. Two patients who received STA-M4 (distal part of MCA) bypass surgery are analyzed. Additionally, the other models with different anastomosis angles and sites are constructed by editing a part of original geometries; (i) the STA is turned over from the original site, the M4-part. (ii) the STA is anastomosed vertically to the M4-part. (iii) the STA is anastomosed to the M2-Superior Trunk, (iv) the STA is anastomosed to the M2-Inferior Trunk. These additional models are also analyzed and evaluated in terms of the change of the mass flow rate between the pre- and post-operative model. In the M4-part anastomosis models, there is a little change in mass flow rate between the differences of anastomosis angle. In the contrast, mass flow rate of the M2-part anastomosis increases at more branch arteries than that of the M4-part anastomosis. This may means M2 anastomosis could be more effective than that of M4 anastomosis.*

1 INTRODUCTION

There are some kinds of cerebrovascular diseases with high mortality and morbidity rate, which are generally called “stroke”. Stroke is classified into three categories; “Intracerebral Hemorrhage (blood vessel ruptures occurred in brain)”, “Subarachnoid Cerebral Hemorrhage (bleeding under arachnoid mater)”, and “Cerebral Infarction (Brain blood flow blockage by thrombus)”. Cerebral Infraction (CI) is generally known as one of the most major cause of death. CI occur from occlusion of cerebral arteries, and oxygen and nutrition decreases, this results in brain necrosis. One major cause of CI is atherosclerosis. And other major cause is occlusion by the thrombus from remote site (e.g. from heart arrhythmia) [1].

One of basic therapeutic method for CI is medical therapy using antiplatelet or anticoagulant. In case those medicines are not effective and its stenosis is very severe or already occluded, surgery may be effective for the prevention of recurrence of the CI.

This surgery is known as revascularization, which can be classified into two methods. One is called Carotid Endarterectomy and Carotid Artery Stenting, these are performed in Cervical Carotid Artery Stenosis and Occlusion, and another is known as cerebrovascular bypass operation. In our study, we focus on the latter one.

STA-MCA anastomosis is one of the bypass surgery to prevent CI. In this operation, the STA (Superficial Temporal Artery) is anastomosed to the MCA (Middle Cerebral Artery), and this results in increase of perfusion of cerebral arteries [2]. Although the bypass operation including STA-MCA anastomosis is performed for many years, there is no evidence of its effectiveness. JET (Japanese EC/IC Bypass Trial) study, conducted in Japan, and COSS (Carotid Occlusion Surgery Study), conducted in North America, are the representative examples. While it was proved that the bypass operation was effective for the CI recurrence prevention in the JET study [3], the COSS study denied it [4]. Therefore, this surgery is still controversial. Furthermore, its operative manners are not well sophisticated, for example, the anastomosis angle and bypass sites.

Therefore, we investigate the relation between the anastomosis condition (anastomosis angle and site) and the brain perfusion, by using CFD. The ultimate objective of this study is to predict the perfusion effects of anastomosis before the operation. In the present study, numerical simulation of blood flow through the patient-specific cerebral arteries with STA-MCA anastomosis is performed. Patient-specific geometries as computational domains are reconstructed from patients’ DSA (Digital Subtraction Angiography) images. In consequence, the post-operative mass flow rate hardly change with changing anastomosis angle compared with the pre-operative one for both cases. The mass flow rate of the M2-part anastomosis increases at more branch arteries than that of the M4-part anastomosis. These results suggest that the pattern of M2 anastomosis could be more effective than that of M4 anastomosis.

2 MATERIAL AND METHODS

2.1 Patient

The information about the analyzed patients was shown in Table 1. Two cases (“Case1” and “Case2”) were analyzed. These patients underwent STA-MCA anastomosis (Single-bypass) at the M4 parietal region for prevention of CI from ICA occlusion.

Table 1: Bypass patients information

Patient	Case1	Case2
Sex	Male	Female
Age	67-years	64-years
Diagnosis	Left-ICA Occlusion	

2.2 Geometric model

At first, post-operative three dimensional data was extracted from patient's DSA (Digital Subtraction Angiography) images taken after the anastomosis operation using medical visualization software "Real INTAGE (Cybernet Systems Co., Ltd., Tokyo, Japan)", and the geometric data of the vascular lumen was obtained. The analysis domain and the name of each branch artery is shown in Fig. 1 and Fig. 2. The geometries with each anastomosis condition are also shown in Fig. 3 and Fig. 4. The extracted data was converted into STL (Standard Triangulated Language) format data, and smoothed using 3D visualization software, "Amira 5.6 (FEI/VSG-division, Bordeaux, France)". Additionally, other geometries changed the STA anastomosis angle and site were made respectively. For the former ones, only the anastomosis angle was changed, and the anastomosis site of the STA was the same as the original one; (i) the STA was turned over from the original site at the M4 and anastomosed. (ii) the STA was anastomosed vertically at the M4-part. For the latter ones, the anastomosis site was changed to the M2-part (proximal to M4 region); (iii) the STA was anastomosed at the M2-Superior Trunk, (iv) at the M2-Inferior Trunk.

To compare the post-operative result with the pre-operative result, the 3D pre-operative lumen geometry was made by editing the post-operative one, because the DSA images of pre-operation did not exist for both patients.

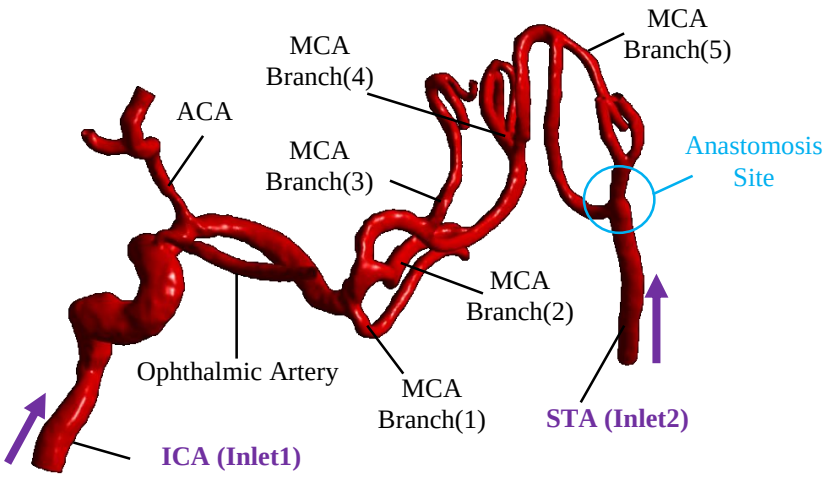

Figure 1: Computational vascular lumen geometry with the post-operation (Case1)

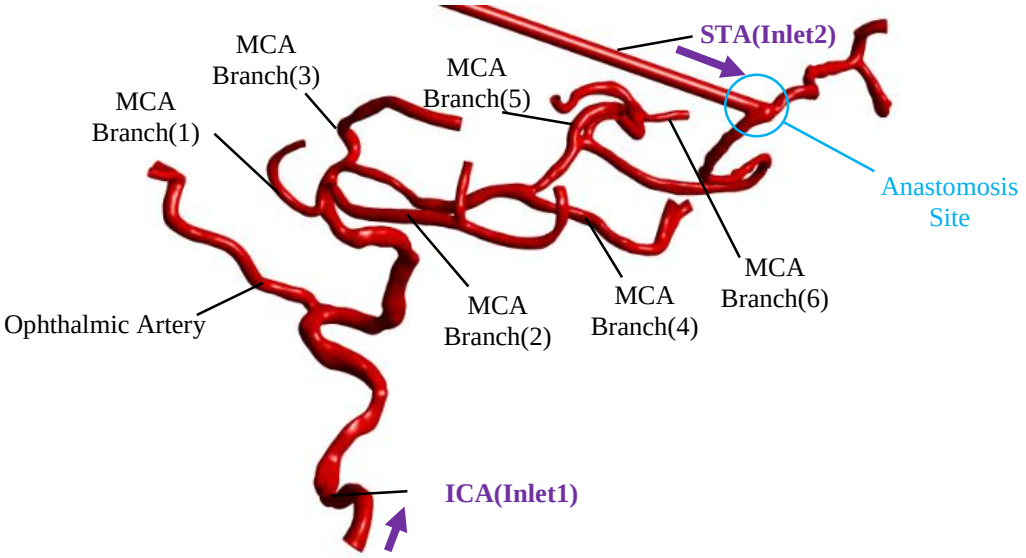

Figure 2: Computational vascular lumen geometry with the post-operation (Case2)

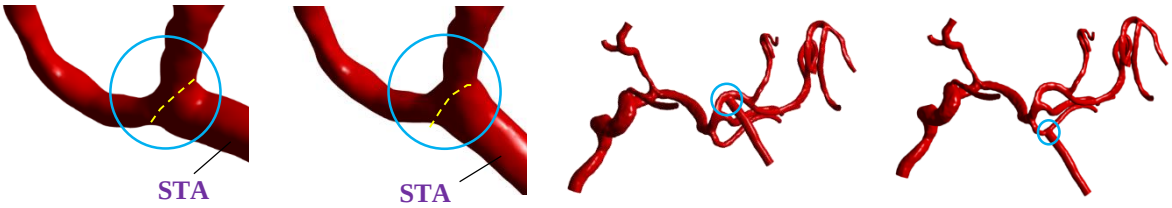

(i) Reverse angle (ii) Vertical angle (iii) M2-Superior Trunk (iv) M2-Inferior Trunk

Figure 3: Computational vascular lumen geometry with each anastomosis condition (Case1)

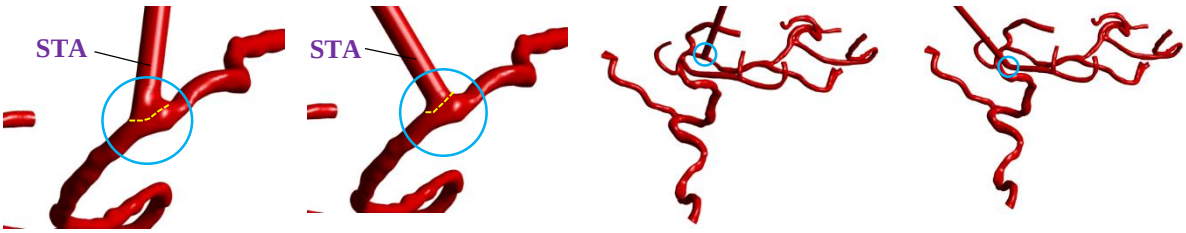

(i) Reverse angle (ii) Vertical angle (iii) M2-Superior Trunk (iv) M2- Inferior Trunk

Figure 4: Computational vascular lumen geometry with each anastomosis condition (Case2)

2.3 Computational mesh

The computational mesh was created based on the STL format data by using "ANSYS ICEM CFD 15.0 (ANSYS, Inc., Canonsburg, PA, USA)". The prism mesh was created along the vascular wall in order to solve boundary layer efficiently, and the tetra mesh was applied to the other region. A number of element was 3.5 million – 4.5 million. To avoid any non-physical solution affected by inlet and outlet boundary conditions, a direct pipe of 75 mm was connected to the inlet and outlet boundaries.

2.4 Inlet boundary condition

For the post-operative model, the inlet boundary condition was imposed to the ICA and the STA. In the present study, mass flow rate of the inlet was calculated by following method called Murray's Law. Generally, blood vessels bifurcate into smaller daughter ones which in turn bifurcate to even smaller ones. The flow satisfies Poiseuille's formula in the parent and all the daughter vessels, and by invoking the principle of minimization of energy dissipation in the flow. The total rate of energy dissipation by flow rate Q in a blood vessel of radius a is equal to sum of the rate at which work is done on the blood, and the rate at which energy is used up by the blood vessel by metabolism. Finally, the following optimal relationship, $Q \sim a^3$ was obtained [6,7],

$$Q_0 = Q_1 + Q_2 \propto a_0^3 = a_1^3 + a_2^3. \tag{1}$$

Where the index of 0, 1 and 2 means a parent vessel and daughter vessels which bifurcated from the parent one, respectively. By using this law, the average mass flow rate of the CCA (Common Carotid Artery), which was obtained from the article of Hoi et al.[5], was distributed to the ICA and the STA, following by the ECA (External Carotid Artery) bifurcation structure and radius of each patients. Their bifurcation structure and radius were measured from 2D-DSA images.

In addition to the "post-operative model", the "pre-operative model" and the "healthy model" were made to evaluate the effect of this operation. Both models used the 3D pre-operative lumen geometry, and the difference between these two models was only inlet boundary condition.

The pre-operative model has the inlet boundary only at the ICA because the STA was not anastomosed. The inlet boundary condition imposed to the ICA was the same mass flow rate as the post-operative model.

To make the healthy model, the healthy condition was defined. This condition was assumed that there was no occlusion at the ICA, and the average mass flow rate of the ICA from the article of Hoi et al. [5] was imposed at the inlet boundary.

2.5 Other computational conditions

In the flow field, laminar flow was assumed since the Reynolds number based on the blood vessels diameter was around 500. At the outlet boundary pressure was fixed to 0 Pa. Rigid and non-slip boundary conditions were assumed on all the vascular wall. The blood was assumed to be a Newtonian fluid with density and viscosity of 1,100 kg/m^3 and 0.0036 Pa·s, respectively. The unsteady flow analysis was performed over two heartbeats (1.8 sec) with a time step of 5×10^{-4} sec. The used solver was "ANSYS CFX 15.0 (ANSYS, Inc., Canonsburg, PA, USA)". In this solver, a node-based finite volume method is adopted. The governing equations are the continuity and the Navier-Stokes equations which are expressed in Einstein summation convention, i.e.

$$\frac{\partial \rho}{\partial t} + \frac{\partial (\rho \boldsymbol{u}_i)}{\partial \boldsymbol{x}_i} = 0, \tag{2}$$

$$\frac{\partial (\rho \boldsymbol{u}_i)}{\partial t} + \frac{\partial (\rho \boldsymbol{u}_j \boldsymbol{u}_i)}{\partial \boldsymbol{x}_j} = -\frac{\partial P}{\partial \boldsymbol{x}_i} + \frac{\partial}{\partial \boldsymbol{x}_j}\left\{\mu\left(\frac{\partial \boldsymbol{u}_i}{\partial \boldsymbol{x}_j} + \frac{\partial \boldsymbol{u}_j}{\partial \boldsymbol{x}_i}\right)\right\}. \tag{3}$$

Where x_i (i=1,2,3) are the Cartesian coordinate. The variable t, u_i and P denotes time, velocity

and pressure, respectively. The physical property ρ and μ denotes density and viscosity respectively. The four equations were integrated over each control volume.

2.6 Evaluation method

To evaluate the effect of anastomosis, we defined the following parameters. *RDH* (Relative Difference to Healthy) was defined to measure how the mass flow rate at each branch arteries, defined as *MFR* (Mass Flow Rate) kg/s, were close to the one of healthy model; i.e. this represents the degree of improvement for an ischemia, expressed in Eqs. (4). Also, *MFGR* (Mass Flow Growth Rate) represents the increase rate of *MFR* against the result with pre-operative model, expressed by Eqs. (5).

$$RDH \equiv \frac{MFR_{post} - MFR_{healthy}}{MFR_{healthy}} \tag{4}$$

$$MFGR \equiv \frac{MFR_{post} - MFR_{pre}}{MFR_{pre}} \tag{5}$$

Where, MFR_{pre}, MFR_{post} and $MFR_{healthy}$ mean the *MFR* with the pre-operative model, with the post-operative model, and with the healthy model, respectively.

3 RESULTS AND DISSUCUSSION

3.1 Velocity distribution

The velocity distributions of each patients are shown in Fig. 5 and Fig. 6. In Case1 (Fig. 5), the post-operative velocity at the M4-part obviously increased compared with the pre-operative one, because the STA supplied with the blood flow. On the other hand, in Case2 shown Fig. 6, the velocity distribution did not change so much between the pre-operative model and the post-operative model.

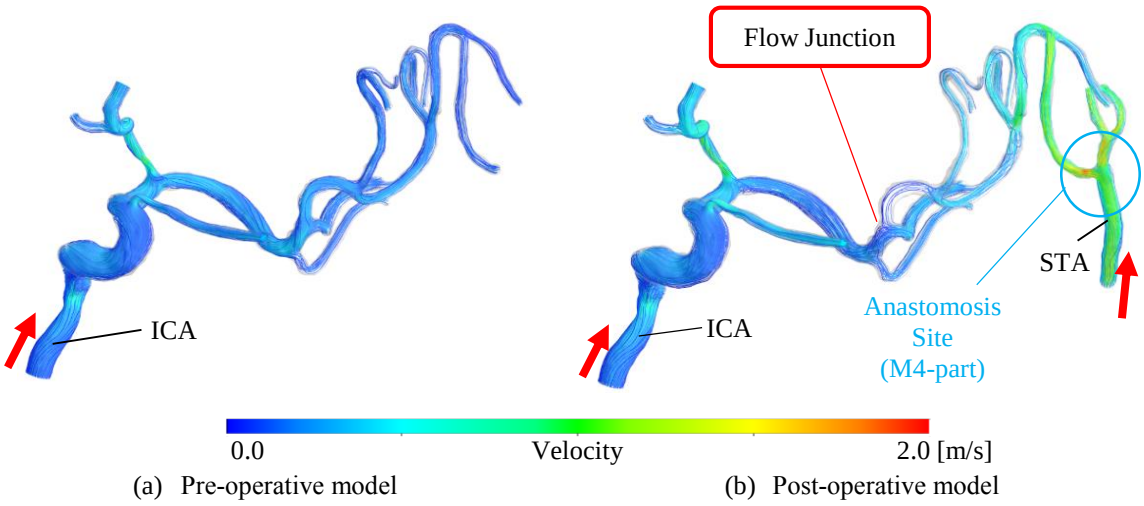

Figure 5: Velocity distribution of the original model (Case1)

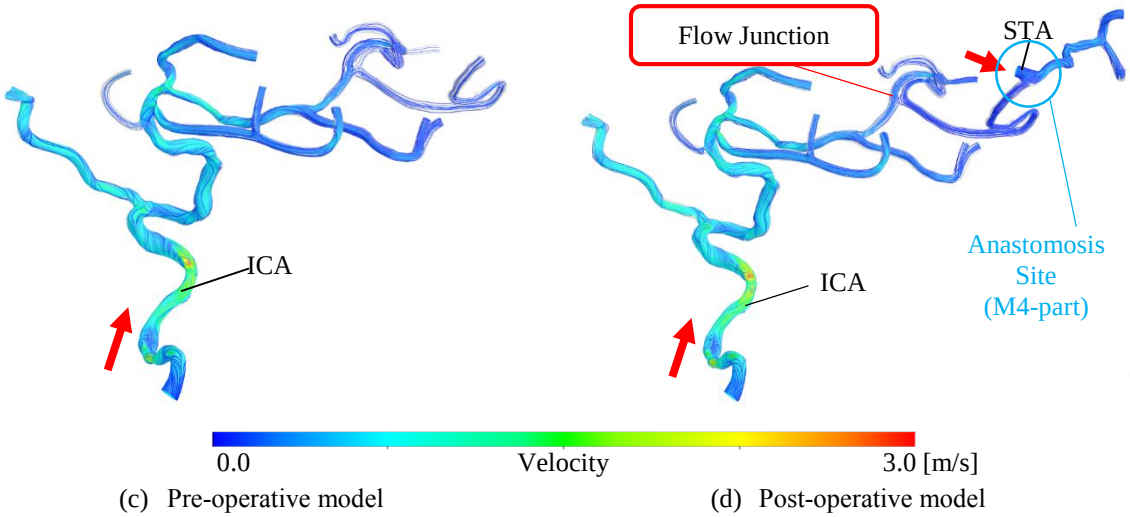

Figure 6: Velocity distribution of the original model (Case2)

3.2 *MFGR* and *RDH*

MFGR and *RDH* at each branch artery in both patients are shown in Table 2, and negative *RDH* values were denoted in boldface letter. Here, the region including the branch arteries (Ophth.A ~ MCA.Br.(6)) and the M4-part are known as the MCA proximal region and the distal region, respectively. At the distal region, the risk of stroke would be high when *MFR* is less than the 80 % of the mean *MFR* of healthy people, as known hemodynamic cerebral ischemia Stage II [8]. In the MCA distal region (M4-part), *RDH* was the positive in both patients, which means their *MFR* exceeded the 80 % of one with the healthy model. In this region, the risk of stroke is expected to decrease with the bypass operation. Switching our attention to the MCA proximal region, *RDH*s were negative at the Ophth.A~MCA.Br.(2) in Case1, the Ophth.A~MCA.Br.(3) in Case2, respectively. Negative *RDH* means that MFR_{post} was less than $MFR_{healthy}$. It may suggest that the operative effect was not sufficient and the risk of stroke might remain.

Table 2: *MFGR* and *RDH* values at each branch of the original model

Region	Branch Arteries Name	Case1		Case2	
		MFGR[%]	*RDH*[%]	*MFGR*[%]	*RDH*[%]
MCA Proximal	Ophth.A	36.9	**-22.1**	1.1	**-16.7**
	ACA	34.7	**-13.5**		
	MCA.Br.(1)	58.9	**-10.3**	2.2	**-12.0**
	MCA.Br.(2)	61.9	**-9.7**	2.2	**-12.0**
	MCA.Br.(3)	77.4	2.9	3.7	**-12.3**
	MCA.Br.(4)	149.1	43.3	21.6	7.5
	MCA.Br.(5)	294.5	129.8	32.0	16.1
	MCA.Br.(6)			34.0	20.4
Distal	M4-part	1319.0	696.6	425.1	358.6

3.3 Relation between the anastomosis angle and the brain perfusion effect

The results of *MFGR* and *RDH* with changing anastomosis angle was shown in Table 3 and Table 4. As a result, extremely poor differences between the original model and model (i), (ii) were obtained; i.e. *RDH* at the same branch artery remained negative in both patients.

Then, the *RDH* results and the flow distribution at anastomosis site (M4-part) were compared for three angle patterns. In consequence, the similar tendency was observed between the *RDH* results and the retrograde blood stream which is the flow provided from the anastomosis site to the MCA proximal region. In Case1, the values of retrograde flow distribution shown in Fig. 7 were 40% (original angle), 43% (pattern (i)), and 42% (pattern (ii)), respectively. In Case2, these values shown in Fig. 8 were 12% in all angle patterns. It means that the retrograde *MFR* hardly changed by altering the STA anastomosis angle, and it would induce the poor change of *MFGR* and *RDH*.

Table 3: *MFGR* and *RDH* values at each branch with different condition of anastomosis angle (Case1)

Region	Branch Arteries Name	**(i) Reverse angle**		**(ii) Vertical angle**	
		MFGR[%]	*RDH*[%]	*MFGR*[%]	*RDH*[%]
MCA Proximal	Ophth.A	39.6	**-20.5**	41.5	**-19.5**
	ACA	36.4	**-12.4**	36.5	**-12.3**
	MCA.Br.(1)	64.1	**-7.4**	63.1	**-7.9**
	MCA.Br.(2)	63.9	**-8.6**	61.4	**-10.0**
	MCA.Br.(3)	88.3	9.3	85.6	7.7
	MCA.Br.(4)	161.9	50.7	158.0	48.4
	MCA.Br.(5)	323.5	146.8	318.8	144.0
Distal	M4-part	1240.4	652.4	1257.5	662.0

Table 4: *MFGR* and *RDH* values at each branch with different condition of anastomosis angle (Case2)

Region	Branch Arteries Name	**(i) Reverse angle**		**(ii) Vertical angle**	
		MFGR[%]	*RDH*[%]	*MFGR*[%]	*RDH*[%]
MCA Proximal	Ophth.A	1.4	**-16.4**	0.8	**-16.9**
	MCA.Br.(1)	-0.5	**-14.3**	1.5	**-12.6**
	MCA.Br.(2)	4.5	**-10.0**	4.4	**-10.1**
	MCA.Br.(3)	3.5	**-12.4**	3.2	**-12.7**
	MCA.Br.(4)	21.0	6.9	21.1	7.0
	MCA.Br.(5)	32.1	16.2	32.0	16.1
	MCA.Br.(6)	32.8	19.3	34.9	21.2
Distal	M4-part	421.0	355.0	423.0	356.8

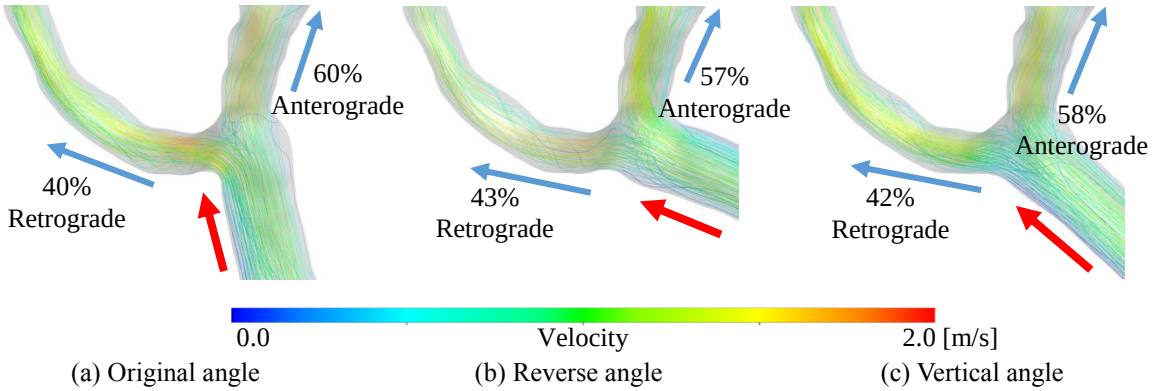

Figure 7: Velocity distribution at the anastomosis site (Case1)

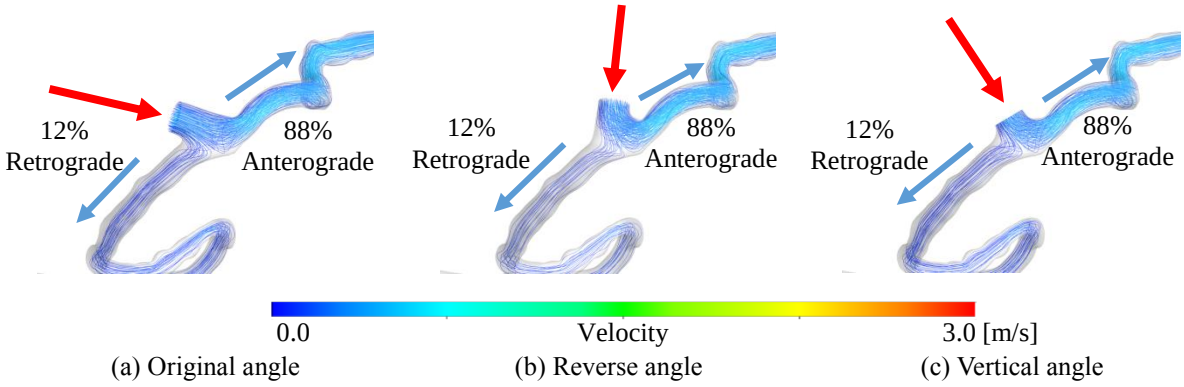

Figure 8: Velocity distribution at the anastomosis site (Case2)

3.4 Relation between the anastomosis site and the brain perfusion effect

The results of *MFGR* and *RDH* with M2-part anastomosis were shown in Table 5 (Case1) and Table 6 (Case2). In Case1, the results of model (iii) and (iv) denote that *MFGR* at Ophth.A ~ MCA.Br.(2) increased by more than 2.5 times compared with the original pattern. As a result, *RDH* at all branch arteries became positive. In Case2, *RDH* at all the branch arteries except Ophth.A were positive, and *MFGR* increased by more than 6.0 times at Ophth.A ~ MCA.Br.(3) compared with the original one. The reason why *MFGR* of (iii) and (iv) were higher than that of the original post-operative model was that STA flow can perfuse the entire MCA system togather with the anterograde ICA flow. In the original pattern, the retrograde flow distribution in Case2 was only 12% and so the STA blood flow could not perfuse to the MCA proximal region, because the STA and the ICA flows were confluent and flowed out for a distal region (Fig. 6 Flow Junction). Considering these results, the pattern of M2 anastomosis ((iii) and (iv)) could be more effective for more branch arteries compared with that of M4 anastomosis. Considering the relation between anastomosis site and perfused region, Nagata et al. [9] stated clinically that surgeons should operate by M2-anastomosis style to perfuse all branch arteries at the MCA region, since M4-anastomosis style can guarantee to increase perfusion in only one branch artery. Our results shown in Table 5 and Table 6 supported the Nagata's clinical report.

Table 5: *MFGR* and *RDH* values at each branch with different condition of anastomosis site (Case1)

Region	Branch Arteries Name	**(iii) M2-Superior Trunk**		**(iv) M2-Inferior Trunk**	
		MFGR[%]	*RDH*[%]	*MFGR*[%]	*RDH*[%]
MCA Proximal	Ophth.A	108.7	18.8	101.0	14.5
	ACA	91.0	22.7	86.9	20.1
	MCA.Br.(1)	169.8	52.3	366.4	163.3
	MCA.Br.(2)	169.9	50.6	158.0	43.9
	MCA.Br.(3)	200.1	74.1	177.1	60.8
	MCA.Br.(4)	188.8	66.1	165.1	52.5
	MCA.Br.(5)	198.5	73.9	173.1	59.1
Distal	M4-part	186.4	60.8	163.0	47.6

Table 6: *MFGR* and *RDH* values at each branch with different condition of anastomosis site (Case2)

Region	Branch Arteries Name	**(iii) M2-Superior Trunk**		**(iv) M2-Inferior Trunk**	
		MFGR[%]	*RDH*[%]	*MFGR*[%]	*RDH*[%]
MCA Proximal	Ophth.A	8.9	**-10.3**	10.5	**-8.9**
	MCA.Br.(1)	20.3	3.6	23.5	6.3
	MCA.Br.(2)	19.5	2.9	58.8	36.7
	MCA.Br.(3)	32.8	12.3	18.4	0.1
	MCA.Br.(4)	40.3	24.0	18.5	4.8
	MCA.Br.(5)	40.2	23.3	18.5	4.2
	MCA.Br.(6)	44.2	29.6	20.0	7.9
Distal	M4-part	41.9	24.0	18.9	3.9

4 CONCLUSIONS

By using the 3D vascular lumen geometry extracted from each patients who experienced STA-MCA anastomosis, we performed patients-specific CFD for two cases, and summarized the results and discussions as follows.

- In all the anastomosis condition (angle and site), *MFR* with the post-operative models are more than 80% of *MFR* with the healthy model at the distal region. This result suggests that the risk of stroke would decrease.
- When surgeons perform this operation by using M4-anastomosis form, the influence on *RDH* and *MFGR* by changing anastomosis angle is little and could be ignored.
- When surgeons perform this operation by using M2-anastomosis form, *RDH* is likely to be positive in the large region, from the MCA proximal region to the distal region, compared with the pattern of the M4-anastomosis.

REFERENCES

[1] Kubota, S. *To study the cerebrovascular disease* (in Japanese). Nagai bookshop, (2009).

[2] Newell, D.W. and Vilela, M.D. Superficial Temporal Artery to Middle Cerebral Artery Bypass. *Skull base* (2005) **15**:133-141.

[3] JET Study Group. Japanese EC-IC Bypass Trial (JET Study): The Second Interim Analysis. *Surg. Cereb. Stroke* (2002) **30**:434-437.

[4] Powers, W.J., Clarke, W.R., Grubb, R.L., Videen, T.O., Adams, H.P. and Derdeyn, C.P. Extracranial intracranial bypass surgery for stroke prevention in hemodynamic cerebral ischemia: The Carotid Occlusion Surgery Study randomized trial. *JAMA* (2011) **306**:1983-1992.

[5] Hoi, Y., Wasserman, B.A., Xie, Y.J., Najjar, S.S., Ferruci, L., Lakatta, E.G., Gerstenblith, G. and Steinman, D.A. Characterization of volumetric flow rate waveforms at the carotid bifurcations of older adults. *Physiol. Meas* (2010) **31**:291-302.

[6] Kamiya, R. *Biomechanics of the circulatory system* (in Japanese). Corona Publishing, (2005).

[7] Kundu, P.K., Cohen, I.M. and Dowling, D.R. *Fluid Mechanics Fifth Edition*. Academic press, (2011).

[8] Nakagawara, J., Kamiyama, K., Usui, R., Takeda, R. and Nakamura, H. The significance of CBF measurements for precise management of carotid stenosis. *J. Neurosurg* (2002) **11**:806-812.

[9] Nagata, S., Sakata, S., Matsuno, H., Yuhi, F. and Ohta, M. Operative indication and technical aspects of the superficial temporal artery to the middle cerebral artery anastomosis: Focusing on the anastomosis to the insular segment of the middle cerebral artery. *Surg. Cereb. Stroke* (1998) **26**:311-317.